JTTEE5 21:695–705
DOI: 10.1007/s11666-011-9725-y
1059-9630/$19.00 © ASM International

Spraying of Metallic Powders by Hybrid Gas/Water Torch and the Effects of Inert Gas Shrouding

T. Kavka, J. Matějíček, P. Ctibor, and M. Hrabovský

(Submitted September 15, 2011; in revised form December 8, 2011)

A hybrid DC arc plasma torch, combining water and gas stabilization, offers a high flexibility in plasma characteristics. These can be controlled in a wide range by the torch operational parameters, such as arc current and secondary gas flow rate. In this study, their influence on plasma spraying of tungsten and copper was investigated. To suppress the in-flight oxidation of the metals, inert gas shrouding was applied. In-flight particle diagnostics and analysis of free-flight particles and coatings was performed for spraying experiments in the open atmosphere and with argon shrouding. Both in-flight particle behavior and coating properties were found to be sensitive to the torch parameters. The application of shrouding was found to affect particle in-flight parameters, reduce the oxide content in the coatings and generally improve their properties, such as thermal conductivity. However, a different degree of these effects was observed for copper and tungsten.

Keywords copper, gas shroud, hybrid water-gas plasma torch, plasma facing materials, plasma spraying, tungsten

1. Introduction

Plasma sprayed coatings provide surface protection/enhancement in a wide variety of applications. Properties of the coatings depend both on the chosen feedstock material and the structure of the sprayed coating. The latter can be to a large extent controlled by plasma spraying parameters, such as torch power, plasma gas type, powder injection conditions, spraying pattern, etc. The flexibility of the spraying parameters offers on one hand the possibility to tailor the properties of the coatings for the desired application; on the other hand, this also necessitates a complex study on the influence of these parameters on the coating structure and properties. These can be traced by so-called 'process maps' (Ref 1), linking the spraying parameters to particle in-flight characteristics and those in turn to the relevant properties of the deposits.

Besides undergoing phase changes (melting in the plasma and rapid solidification upon impact), the sprayed material may also experience chemical changes. A typical example is oxidation, which inevitably occurs during spraying of metals in the open atmosphere, when the hot particles come in contact with oxygen from the air. The presence of oxides in the coatings can have a significant influence on their properties (Ref 2); therefore, the oxidation process has been subject to extensive research, including ways to suppress it. Among these are shrouding of the plasma jet by inert (Ref 3) or reactive gas (Ref 4) or spraying in a closed chamber with controlled atmosphere or vacuum (Ref 5).

Tungsten-based coatings represent an example of material where oxidation during spraying is important. They can find a use in various thermal management applications, such as thermonuclear fusion. Tungsten, with its refractive nature, can provide a plasma facing surface in a Tokamak, where it would be subjected to large heat and particle fluxes, and thereby protect the underlying components (Ref 6). Copper, with its high thermal conductivity, represents a suitable candidate material for heat removal. Combination of these coatings (Ref 7) offers a prospective alternative to bulk material processing, which is particularly difficult in the case of tungsten.

Both materials have been sprayed by water stabilized plasma, among other techniques. Relatively low thermal conductivity, caused by the porosity and presence of oxides, has been identified as the main hindrance to successful application. Among the attempts to suppress the in-flight oxidation were auto-shrouding by admixture of WC to W powder and traditional shrouding of the jet by inert or reactive gas (Ref 8). In both cases, the effect was positive, but small. Initial experiments with a hybrid torch

This article is an invited paper selected from presentations at the 2011 International Thermal Spray Conference and has been expanded from the original presentation. It is simultaneously published in *Thermal Spray 2011: Proceedings of the International Thermal Spray Conference*, Hamburg, Germany, September 27-29, 2011, Basil R. Marple, Arvind Agarwal, Margaret M. Hyland, Yuk-Chiu Lau, Chang-Jiu Li, Rogerio S. Lima, and André McDonald, Ed., ASM International, Materials Park, OH, 2011.

T. Kavka and **M. Hrabovský**, Institute of Plasma Physics, Thermal Plasma, Prague, Czech Republic; and **J. Matějíček** and **P. Ctibor**, Institute of Plasma Physics, Materials Engineering, Prague, Czech Republic. Contact e-mail: kavka@ipp.cas.cz.

(Ref 9), which uses a mixture of water and argon as plasma-forming media, showed promising improvements in tungsten coating properties (Ref 8). These were attributed to lower exit temperature of the jet with a lower downstream gradient and more efficient particle acceleration. The above mentioned factors have prompted a more extensive study, part of which is presented in this paper.

In this study, the influence of plasma spraying conditions on the behaviour of metallic powder particles and coating formation has been investigated. The investigations focused on two aspects: variation of the parameters of the hybrid torch and the application of a newly designed shrouding system.

2. Experimental Setup

The configuration of the plasma torch is shown in Fig. 1. The torch consists of three main parts: a cathode part, a water stabilized part and an anode. The cathode part is designed in the same way as in gas torches. Argon is supplied tangentially along the tungsten cathode and argon plasma flows through the cathode nozzle into the water stabilized part, where the arc column burns inside the water channel. Here a principle of Gerdien arc is utilized. Water is tangentially supplied at three positions along the arc chamber under high pressure to form a vortex. Heat released by the arc causes evaporation of water from the inner surface of the vortex and the steam is mixed with the argon plasma, heated and ionized. The overpressure existing inside the arc chamber results in the formation of a fast high-temperature plasma jet at the torch nozzle. The anode is created by a rotating copper disk positioned outside the torch downstream of the jet. Both electrodes are water-cooled. The specific design of the torch provides formation of a rather long arc, more than 50 mm in length. The plasma torch is characterised by rising volt-ampere characteristics and can work at arc power up to 180 kW for arc current up to 600 A. In this study, arc current varied between 300 and 500 A, while the argon flow rate was varied between 12 and 36 slm. For these conditions, the torch total power was in the range 60-135 kW and the torch thermal efficiency was 50-65 %.

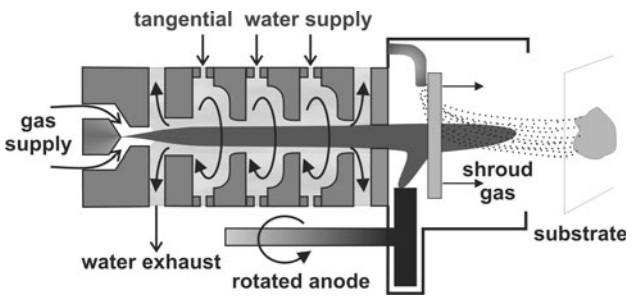

Fig. 1 Schematic diagram of the plasma torch and spraying process

Two powders were used in the present experiments: copper powder (Stamont Metal International, Slovakia) with granulometry between 100 and 125 μm and tungsten powder (Alldyne Powder Technologies, USA) with granulometry between 63 and 80 μm. The powder particles were injected transversally into the plasma jet through a single injector under 70° angle to the torch axis at three feeding distances (FD): 25, 60 and 90 mm from the torch nozzle. The choice of FD was dictated by the properties of the used materials and entrances available in the shielding system. Refractory tungsten was injected closer to the torch (25 and 60 mm), where the plasma jet is still very hot. Copper, which has low melting point, was injected at farther distances (60 and 90 mm). Argon was used as a carrier gas, with a flow rate of 5-5.9 slm (slightly varied depending on powder and torch parameters). The powder feed rate was 8.5 and 17.1 kg/h for Cu and 13.5 and 27.1 kg/h for W powder, for particle in-flight characterisation and coating deposition, respectively. Three main parameters, expected to influence plasma-particle interaction, were varied in this study: arc current, feeding distance and flow rate of argon as a secondary plasma-forming gas.

The plasma spraying tests have been carried out under both atmospheric and shrouding conditions. The anode disk positioned immediately after the torch nozzle does not allow application of the typical shrouding nozzles used in spraying or cutting gas torches. For the shrouded plasma spraying, the torch was attached to a specially designed water-cooled shielding tube 280 mm in length, which covered the exit region of the torch together with the anode (Fig. 1). The shroud gas was supplied at two positions: into the anode region through a single port and through the gas distribution ring positioned downstream of the nozzle right after the anode. The shroud gas was distributed with the help of a specially designed gas distribution ring through holes 1 mm in diameter and directed parallel to the torch axis. In most cases, argon was used for shrouding, with a controlled flow rate. The shielding system had a circular opening, through which particles were flying towards the substrate.

In-flight particle parameters were measured by a DPV-2000 system (Tecnar Automation Ltd., Canada) (Ref 10). The system scanned the plane perpendicular to the particle flow at 320 mm distance from the torch nozzle, the location of the substrate in subsequent spraying experiments, to examine particle in-flight parameters just before their impact on the substrate. The system collected data from 60 × 60 mm grid scans at 15 mm steps to ensure obtaining parameters of the whole particle field. The obtained data were then statistically processed in Matlab to obtain mean values of particle temperatures and velocities. Only conditions with sufficient number of captured particles were considered.

Particle in-flight oxidation was also studied. The particles were sprayed into liquid nitrogen to preserve particle in-flight state and separate the in-flight oxidation from that of solidified deposited material. The plasma torch was positioned vertically above a vessel filled with liquid nitrogen in such a way that the distance between the torch

and nitrogen surface corresponded to the spraying distance. The particles were collected during 10-20 s of spraying. The nitrogen level changed during each run due to evaporation. Thus, the average spraying distance was different from the initial one. However, this difference was largely similar across spraying conditions, thus the results reflect general trends in the effect of spraying conditions on particle in-flight oxidation. Oxygen content was determined by the inert gas fusion technique using a Leco TC 500 analyzer (Leco Corp., USA) at Unipetrol RPA.

In-flight particle behaviour was examined for a wide range of parameters, while only a limited number of conditions were selected to produce coatings, to see the main correlations between particle state and coating properties. During the spraying tests, the torch was fixed at a stationary position, while the substrate holder was moved with linear velocity of 300 mm/s. Inert gas shielding was also applied on the substrates to suppress oxidation of the coating surface during the deposition and cooling down phase. The substrates made of grit-blasted copper and carbon steel 2.5 × 25 × 100 mm in dimensions were first preheated to ~100 °C and this temperature was roughly maintained during the deposition, with the help of water flow through the substrate holder. Coatings typically 1 mm thick were deposited during several cycles of a rectangular raster pattern of the torch.

Afterwards, morphological and structural observations of the free-flight particles and coatings were performed in an EVO MA15 scanning electron microscope (Carl Zeiss, Germany) in the backscattered and/or secondary electron mode. Thermal diffusivity and conductivity were determined by the xenon flash method on free standing coating samples, using an FL-3000 instrument (Anter Corp., USA).

3. Results and Discussion

3.1 Effect of Plasma Torch Parameters on Particles in Flight

Modification of the plasma torch parameters results in strong changes of properties of the generated plasma. Change of the arc current and secondary gas flow rate affects plasma composition, power of the generated plasma, plasma jet temperature, velocity and enthalpy. The plasma gas composition varies from almost argon plasma for low arc current and high Ar flow rates to almost water plasma for low Ar flow rate and high arc currents. The effect of plasma torch parameters on plasma enthalpy is shown in Fig. 2. The generated plasma exhibits the highest enthalpy values for low Ar flow rates and high arc currents. Both the increase of argon flow rate and decrease of arc current result in enthalpy reduction. The plasma jet temperature and velocity are also influenced by these parameters: an increase of arc current results in higher plasma temperatures and velocities, while an increase of Ar flow rate affects only plasma velocity. More detailed analysis of the properties of the generated plasma is given in Ref 11.

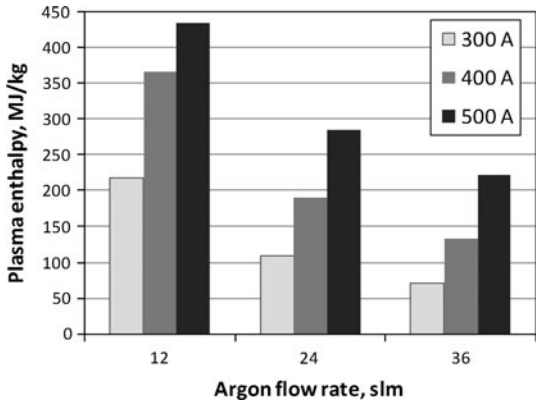

Fig. 2 Plasma enthalpy as a function of plasma torch parameters

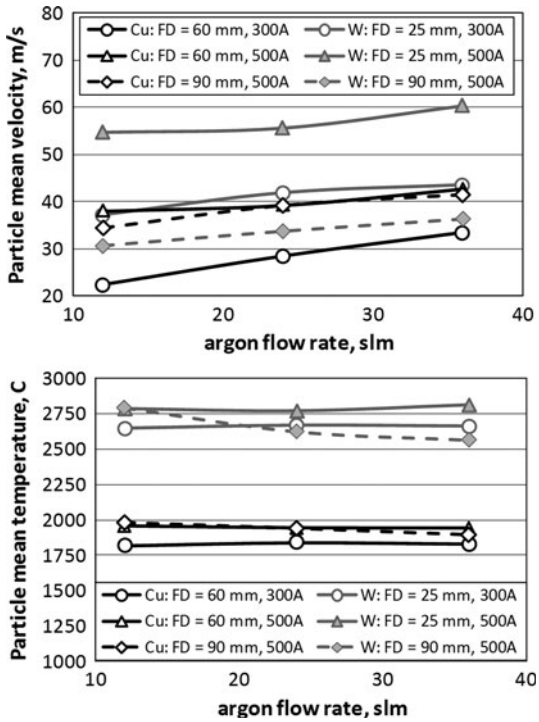

Fig. 3 Effect of plasma torch parameters on particle in-flight behaviour at 320 mm from the nozzle: mean particle velocity and mean particle temperature

The effect of plasma torch parameters on particle in-flight behaviour was studied in a wide range of parameters. Mean values of particle temperature and velocity for different conditions and for both studied powders are shown in Fig. 3. It is obvious that an increase in either arc current or argon flow rate results in an increase of the particle velocity; the current effect is more pronounced. This effect corresponds to changes in the properties of the generated plasma. Indeed, an increase of the arc current leads to an increase of the plasma jet velocity. Argon flow rate has the same effect, which is also accompanied by modification of the plasma jet composition. A higher amount of argon results in an increase of

the plasma viscosity, which improves the momentum transfer between the plasma jet and particles. For the same plasma spraying conditions (FD = 90 mm, I = 500 A) copper showed a little higher velocity values. It is connected to a different particle density and size distribution. The ratio of the drag force (proportional to the cross-sectional area) to the particle inertia (proportional to the particle volume and density) at the same flow conditions is somewhat higher for copper particles. The effect of the spraying parameters on particle temperature was less pronounced. An increase of arc current always resulted in an increase of the measured temperatures. An increase of the argon flow rate almost did not affect temperatures for the shorter FD. However, for longer feeding distances (FD = 90 mm) there was a temperature decrease observed for both materials. In general, temperatures measured during W spraying were much higher than for Cu owing to its higher melting point. The measured temperatures of Cu may be overestimated for low current conditions, as a much smaller amount of particles was evaluated by the system in comparison to the high current conditions. These low-luminosity low-temperature particles were not recognized by the system and thus were not considered. For both materials there was a noticeable evaporation observed during the spraying, which was likely connected to oxidation of the metallic particles due to their reaction with oxygen from the surrounding atmosphere. Indeed, the temperature of boiling for oxides of both materials is much lower than for the pure material (T_b(Cu) = 2500 °C, T_b(W) = 5,700 °C, T_b(CuO) = 2000 °C, T_b(CuO_2) = 1800 °C, T_b(WO_2) = 1730 °C, T_b(WO_3) = 1837 °C) (Ref 12). The measured particle temperatures have also been affected by the evaporation process. The temperatures measured for Cu were much above its melting point (T_m(Cu) = 1085 °C), but varied in the range of values of the boiling point of the copper oxides. It may be caused by a formation of the oxide layer on the molten particle surface, which is continuously evaporated. On the other hand, according to measurements, only a few tungsten particles reached their melting temperature. The average particle temperatures for W were significantly below its melting point (T_m(W) = 3410 °C). However, coatings were produced at these conditions, which indicates that particles had higher temperatures. A similar phenomenon was also observed by Niu et al.13 The temperature measurement might have been affected by the existence of the cloud of oxide vapor, which was formed at much lower temperatures than those measured. More detailed study is necessary to explain the observed phenomena.

The effect of torch net power on particle in-flight temperature and velocity for a whole set of studied parameters is shown in Fig. 4. The feeding distance was 60 mm for copper powder and 25 mm for tungsten. In fact the pictures represent the first order process maps of the hybrid torch. The results illustrate the crucial role of the torch net power on particle characteristics: an increase of the power led to an increase of both particle temperature and velocity. The effect of argon flow rate on particle temperature is negligible. Thus, this reflects a possibility to fix the particle temperature at a desired level by varying the torch net power and then to modify particle velocity and thus the time of particle flight through the plasma by changing the argon flow rate.

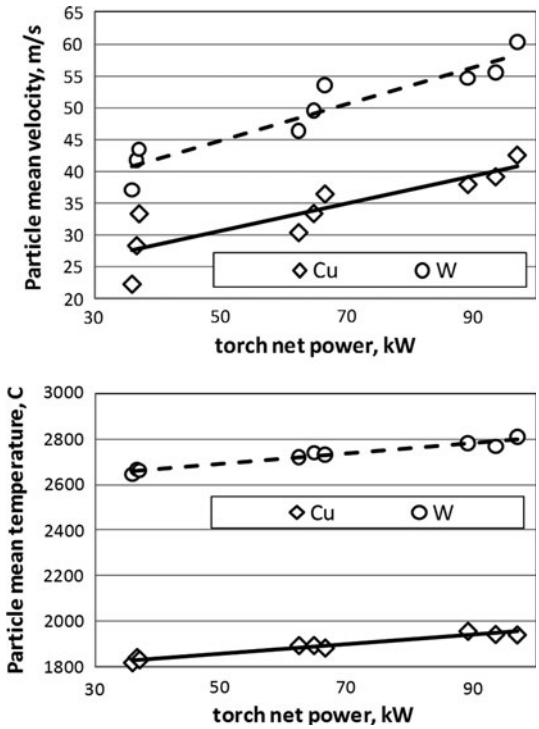

Fig. 4 Effect of torch net power on in-flight particle temperature and velocity at 320 mm from the nozzle: pooled data from all settings

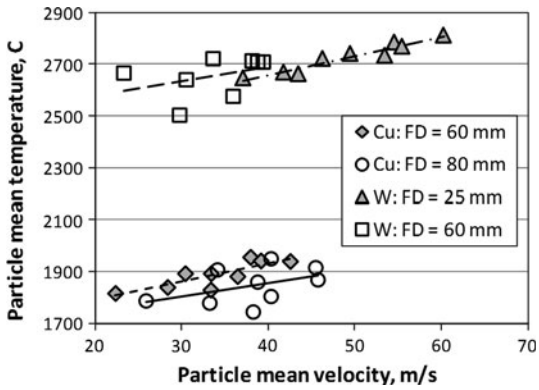

Fig. 5 Correlation between particle in-flight temperature and velocity: pooled data from all settings

Dependence of particle mean temperature on particle mean velocity for two FD for both studied powders is shown in Fig. 5. The data were collected from the whole range of studied settings. Overall, higher particle velocity corresponded to higher temperature. Moreover, slopes of the fitting curves also coincide for both powders despite their different size distribution and material properties for different FD. It seems to be a specific feature of the hybrid torch.

3.2 Effect of Shrouding

As mentioned earlier, during plasma spraying of metallic materials in open atmosphere, their oxidation usually takes place. Molten material interacts with oxygen coming into the jet from the surrounding atmosphere due to entrainment of the ambient air. The spectroscopic measurements have shown that air is present at the plasma jet centerline already at the distance of several centimetres from the nozzle. At the region of the substrate position, the plasma jet consists of mostly air (Ref 14). The presence of oxides may change the properties of the sprayed material and thereby affect the properties of the resultant coatings. To suppress the strong oxidation effects taking place during the particle in-flight phase, a shielding system with a shrouding gas was tested. The particle parameters were measured at 320 mm distance from the torch nozzle at the end of the shielding tube. Argon was used as a shroud gas with a flow rate of 100 slm. The amount of the recorded particles was roughly equal for both conditions. The average particle temperature and velocity and their standard deviations with and without shrouding are shown in Fig. 6 for selected conditions for both materials. The spraying parameters are indicated in the following way: arc current-argon flow rate-feeding distance. The effect of shrouding was different for the illustrated cases. For all the studied conditions, shrouding had a positive effect on velocity distribution as it became narrower. However, there was no obvious effect on mean velocities of Cu particles, and mean velocities of W particles even decreased. The effect of shrouding on the temperature of W particles is not pronounced, while for Cu, the average temperature as well as its deviation increased for shrouding conditions. In general, scattering of measured values was higher for W for all studied conditions.

Oxidation of the particles during their flight through the plasma jet under different conditions was also studied. The results of oxygen content analysis for Cu powder are shown in Fig. 7. The oxygen content in feedstock material was 0.41 wt.%. Modification of the argon flow rate had a large effect on the oxide content: its increase from 12 to 36 slm resulted in a decrease of oxygen content of almost four times. Besides the changed plasma composition, the effect is related to time of particle flight through the flame. According to DPV measurements, particles are faster for higher flow rates and stay a shorter time in the flame. Slower particles are heated to higher temperatures and increased temperatures promote the oxidation process. Despite a higher particle velocity, the oxide level increased with arc current. It may be connected to higher particle temperatures as well as to stronger air entrainment. Indeed, for higher arc currents the entrainment rate is higher (Ref 15). Moreover, the particles injected into hotter regions of the plasma jet (FD = 60 mm) reach higher temperatures and they stay longer in the flame before impact. Thus, they are more oxidized. Application of the shrouding gas (250 slm of argon) resulted in reduction of the oxygen content, which was most pronounced for low argon flow rate conditions. Argon shrouding replaced air from the jet surroundings, thus protecting the particle flow and reducing the amount of oxygen available for oxidation. It should be noted that the oxygen level in particles sprayed with the shrouding was even below the level found in the feedstock material. It may be caused by evaporation of the copper oxides contained in the powder during particle flight through the plasma jet.

For W powder, the original feedstock contained 0.0146 wt.% of oxide. The oxide content after flight through the plasma was around 0.06 wt.% for all studied conditions. It is obvious that the majority of the formed oxides evaporated during particle flight, which was confirmed by a presence of vapor clouds observed during the spraying tests. Thus, application of the shroud gas may

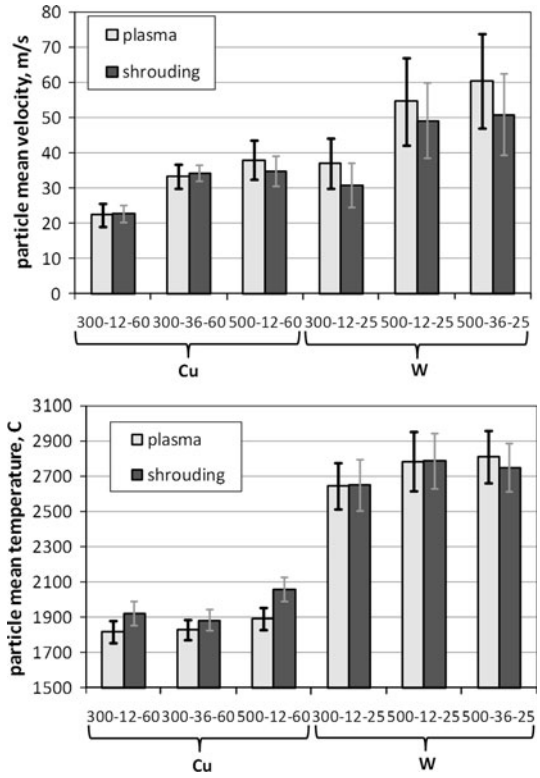

Fig. 6 Effect of gas shrouding on particle in-flight mean velocity and temperature at 320 mm from the nozzle

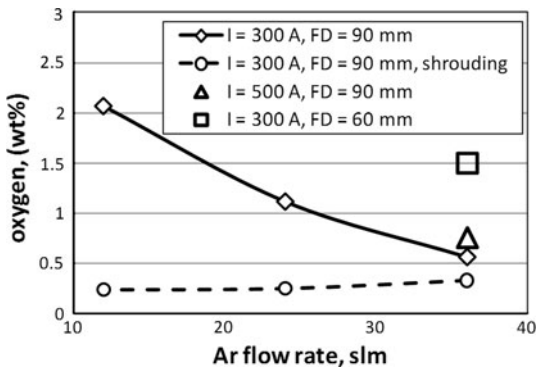

Fig. 7 Oxygen level in Cu particles after their flight through the plasma jet under different conditions

affect the deposition efficiency, but not chemistry of the deposition process. However, it was not in the scope of the present study.

3.3 Splats

At selected parameter settings, isolated splats were collected on polished stainless steel substrates, preheated to ~100 °C, and observed by SEM. They were classified according to their shape and melting degree. The influence of torch parameters on Cu splat shapes was described in Ref 11. Representative W splat shapes and overall splat characteristics are shown in Fig. 8 and Table 1, respectively. The splat types are classified as follows (a letter in brackets corresponds to the micrograph labeling in Fig. 8): A = unmelted or nearly-unmelted (a, left splat in c),

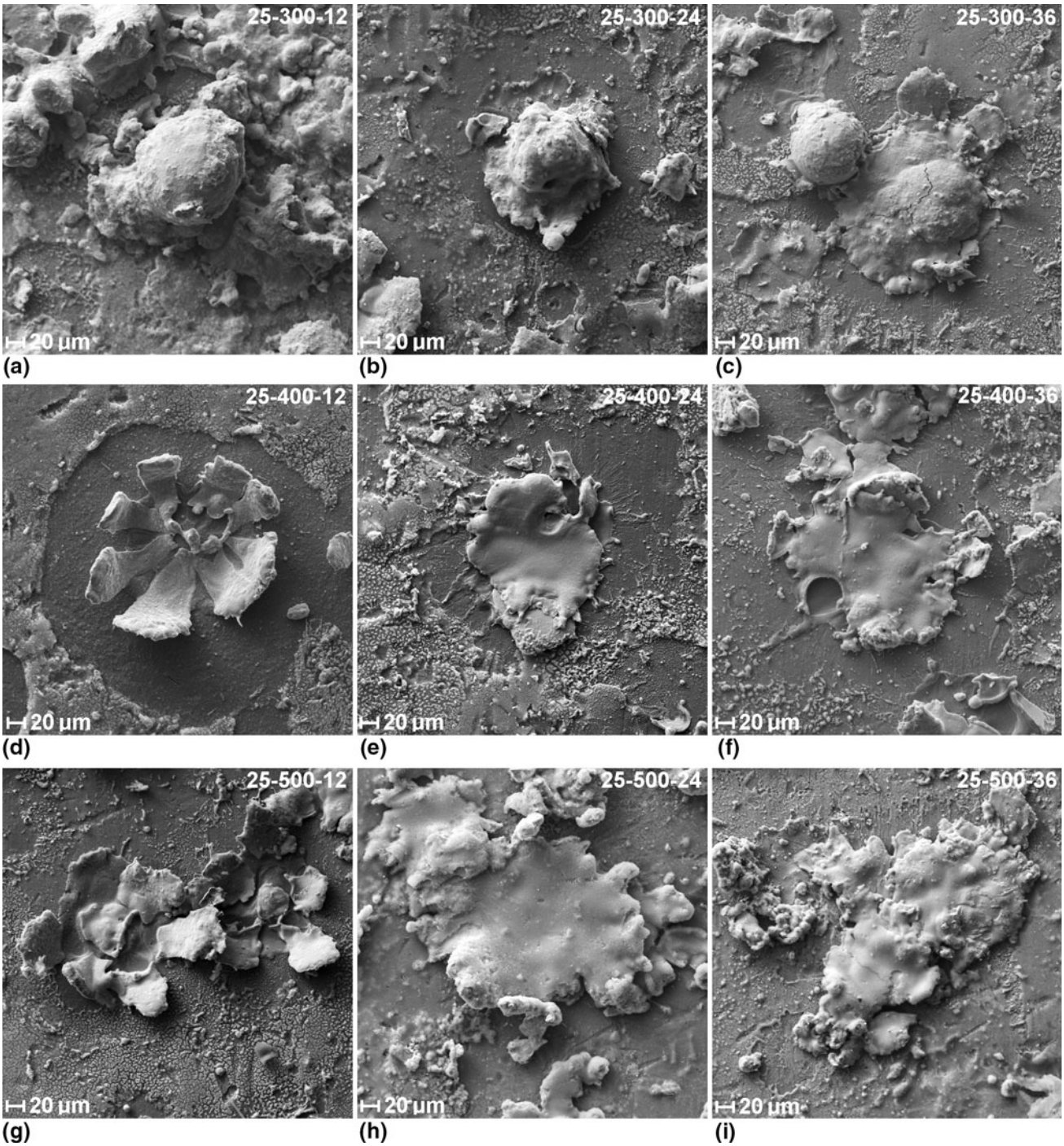

Fig. 8 Typical W splat shapes for various spraying conditions (labeled in the following order: feeding distance – torch current – Ar flow rate). Fine particles around the splats are likely deposits of tungsten oxide evaporated during the flight (Ref 16)

Table 1 Relative occurrence of different types of W splats and overall splat characteristics in dependence on spraying conditions

Spraying parameters			Relative numbers of splats						Splat morphology		
			Splat type						Degree of		
Injector (mm)	Arc current (A)	Argon flow (slm)	A	B	C	D	E	F	Melting	Flattening	Fragmentation
60	300	12	**	*				*	*	*	
60	300	24	*								
60	300	36	*								
60	400	12		*	***	*			*	*	
60	400	24	***	*	*				*		
60	400	36	***	*					*		
60	500	12				**	*	**	***	***	*
60	500	24		**	***	**			**	**	*
60	500	36	**	**		*		**	*	*	*
25	300	12		***	**				*	*	*
25	300	24		**	*			**	**	**	**
25	300	36		**	*			**	**	**	**
25	400	12		*	*			***	***	***	***
25	400	24		*	**		*	**	**	***	**
25	400	36		*	*		**	**	**	***	**
25	500	12		*			**	***	***	***	***
25	500	24					***	**	***	***	**
25	500	36		*	**	***	*	*	***	***	*

The number of asterisks shown in column 2 indicates the relative number of splats of a particular type: *** dominant (majority of the splats were of this type), ** frequent (significant number, but minority), * present (occasional occurrence), *0* absent. In column 3, the asterisks indicate the relative degree of a particular phenomenon/characteristic: *** high (i.e., the splats were completely molten, highly flattened or highly fragmented), ** medium, * low, *0* extremely low or none (i.e., the deposited particles were unmelted, equiaxial, contiguous)

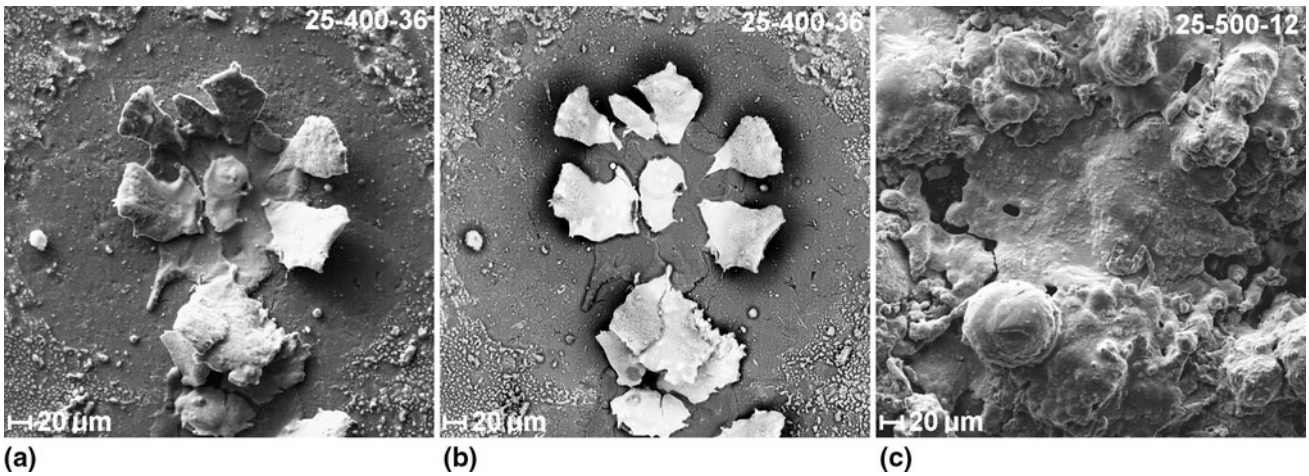

Fig. 9 Detail of a fragmented splat on polished stainless steel substrate, (a) SE image, (b) BE image, and (c) contiguous splat on coating surface

B = partially molten, hemispherical (b), C = semi-molten, moderately flattened (right splat in c), D = semi-molten, well flattened (i), E = well molten, contiguous (e, f, h), F = well molten, fragmented (d, g). Splat types D and E are expected to form the densest coatings. The samples often contained a mixture of various splat types; their relative occurrence and morphology is summarized in Table 1. The number of asterisks corresponding to a particular type of a splat symbolizes their relative number observed at a given condition. The last three columns summarize qualitatively the splat morphology. The number of asterisks in this case reflects the overall degree of melting, flattening and fragmentation. Contrary to copper, where full melting of the particles took place for all conditions, tungsten particles were completely molten only for conditions with high plasma enthalpy, i.e. high torch current and short feeding distance. At medium current (400 A), the degree of melting was slightly reduced with increased Ar flow, as could be expected from Fig. 2. For splats formed from completely molten particles, fragmentation upon impact was frequently observed, leading to flower-like splats (Fig. 9). This is thought to be

connected with substrate melting, evidence of which is seen in Fig. 9(b)), between the W splat fragments. These appear to have glided on a thin layer of liquid steel, whose melting point is much lower than that of tungsten. This phenomenon did not occur in splats impacting on previously deposited tungsten layers—splats observed on the coating surface (Fig. 9(c)) were contiguous. Therefore, is it not expected to have a significant influence on overall coating properties. Increased argon flow has reduced this phenomenon slightly. Only well molten and well flattened splats are expected to form dense coatings (see below). The corresponding torch conditions (towards the bottom of Table 1 and Fig. 8) also led to higher deposition efficiencies.

3.4 Coatings

Figure 10 shows representative Cu coating structures obtained at selected spraying conditions (shown in top right corners), where the effects of different parameters can be illustrated. Figure 10(a) shows a Cu coating sprayed at FD = 90 mm, I = 300 A, Ar = 36 slm, with a typical lamellar structure, small amount of porosity, small degree of oxidation and a few unmelted particles. The coating shown in Fig. 10b, sprayed with higher torch current, exhibits a higher degree of oxidation and better bonding between individual splat layers, both as a result of higher particle temperature. Comparison of Fig. 10(a) and (c) illustrates the effect of argon flow rate. The coating in Fig. 10(c), sprayed with lower argon flow rate, exhibits poorly bonded splats, visible intersplat porosity and higher oxide content than its counterpart in Fig. 10(a). The coating shown in Fig. 10(d) was sprayed at the same torch settings, but with the application of Ar shrouding. Its positive effect is clearly reflected in better intersplat bonding, lower porosity and lower oxide content. All of these factors have a direct influence on the coating properties, such as thermal conductivity, as will be discussed below.

Representative W coating structures are shown in Fig. 11. Because of its refractory nature, tungsten powder

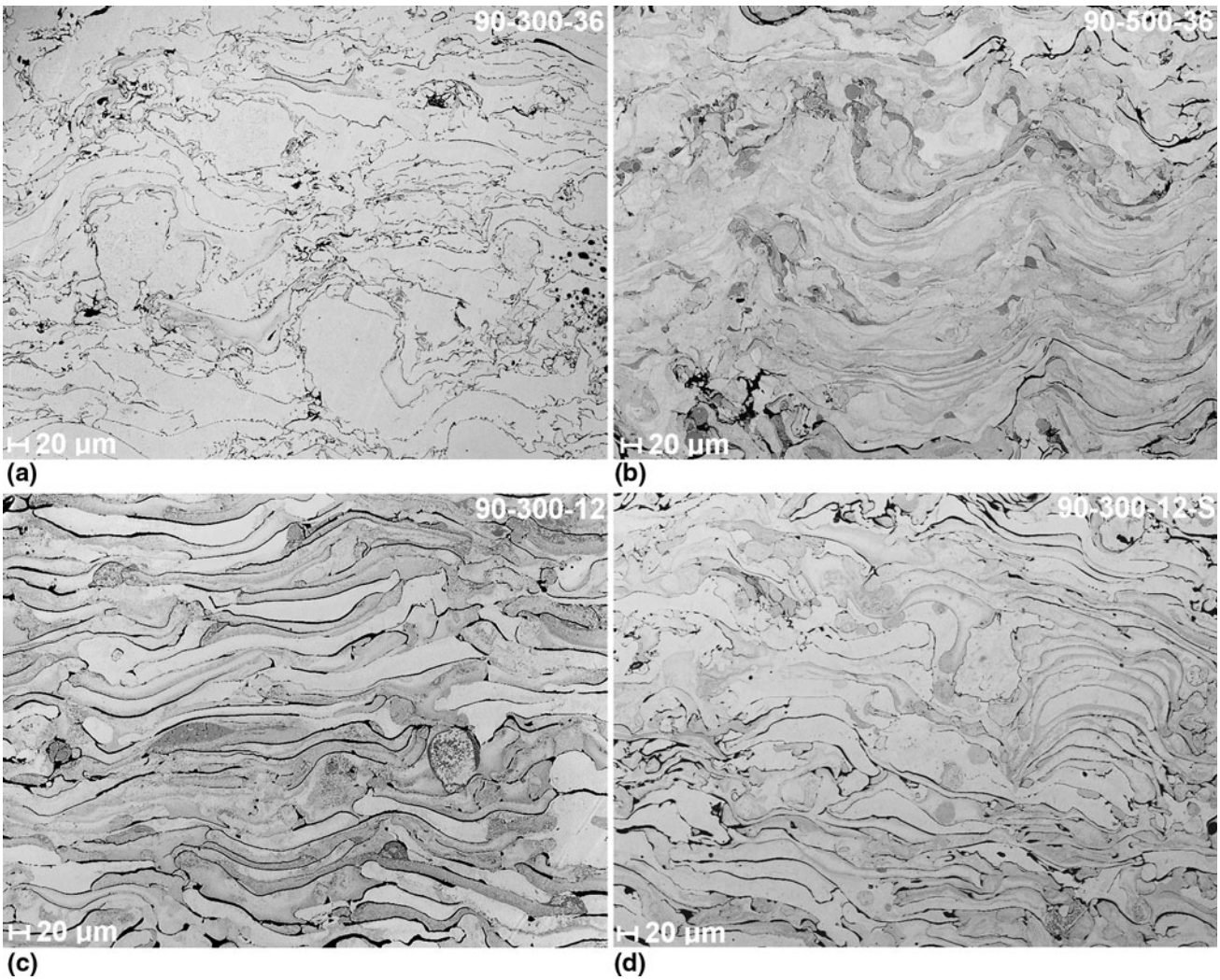

Fig. 10 Typical Cu coating structures in dependence on spraying conditions (labelling: feeding distance – torch current – Ar flow rate, S - shrouding)

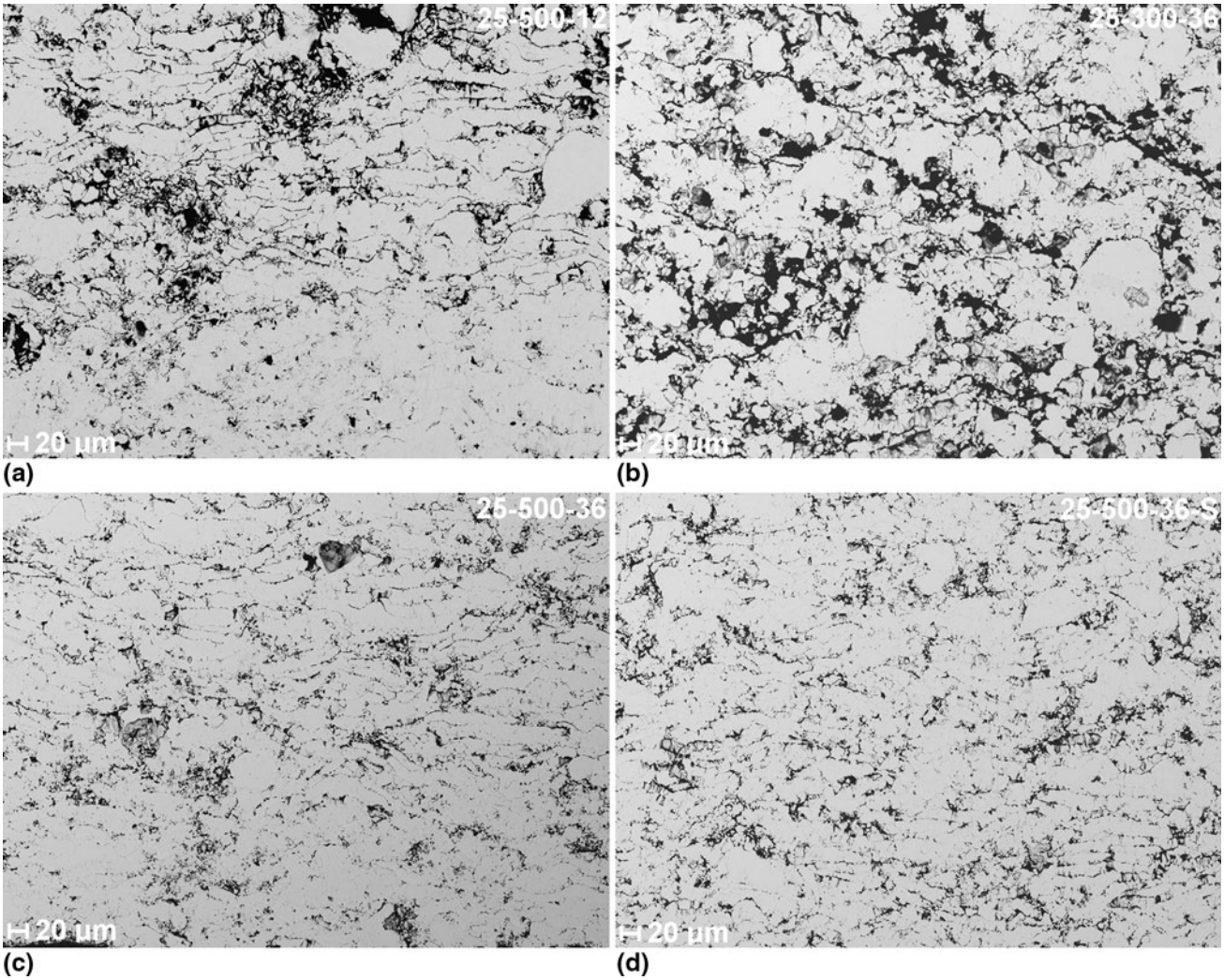

Fig. 11 Typical W coating structures in dependence on spraying conditions (labelling: feeding distance – torch current – Ar flow rate, S - shrouding)

had to be sprayed at higher plasma temperatures (i.e. higher current and shorter feeding distance) than copper, in order to obtain reasonable quality coatings. As discussed above, oxidation takes place during the flight as well, but is accompanied by rapid evaporation of the oxides. As a result, the amount of oxides in the coatings is very small and cannot be discerned as a separate phase. The porosity is generally higher and the layered structure is less distinct than in the case of copper coatings. The use of low current (300 A, Fig. 11(b)) resulted in porous coatings with a noticeable portion of unmelted particles, indicating insufficient plasma enthalpy to properly melt the tungsten powder. Comparison of coatings sprayed at higher current (500 A, Fig. 11a and c) shows again a positive effect of the argon flow rate, where denser coatings were obtained with higher flow rate. Contrary to copper, the application of argon shrouding did not have a pronounced effect on tungsten coatings, as the structures shown in Fig. 11(c) and (d) are very similar.

The microstructural variations, resulting from different spraying conditions, were also reflected in coating properties. Figure 12 shows the effect of argon flow rate on thermal diffusivity and conductivity of copper and tungsten coatings sprayed in the open air. A higher argon flow rate results in more conductive coatings, which could be attributed to lower porosity as well as less oxidation.

The oxygen content in copper coatings is shown in Fig. 13. Reduction in oxygen content with increasing argon flow rate is clearly seen. Similar to free-flight particles, higher particle temperatures (achieved by higher arc current or shorter feeding distance, at the same argon flow rate) resulted in a higher degree of oxidation. Application of shrouding markedly reduced the oxygen content at lower argon flow rates, but both shrouded and unshrouded curves converged at the highest flow rate. The oxygen content in coatings is about 1-1.5% higher than in free-flight particles captured in liquid nitrogen, indicating that the post-deposition oxidation phase is about as significant as the in-flight phase despite usage of the protecting gas.

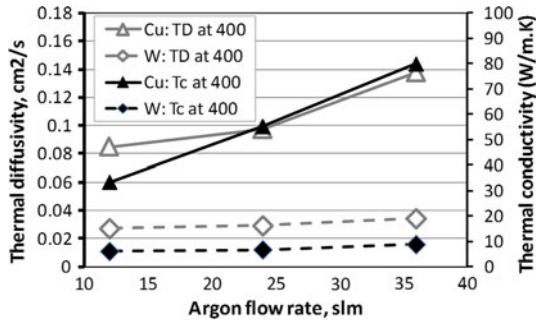

Fig. 12 Effect of argon flow rate on coating properties (for W: FD = 25 mm, I = 500 A; for Cu: FD = 90 mm, I = 300 A). Data measured at 400 °C are shown, but the trends at other temperatures were similar

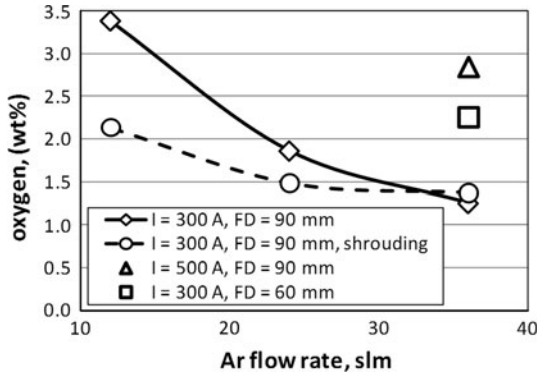

Fig. 13 Oxygen content in Cu coatings for different spraying conditions without and with shrouding

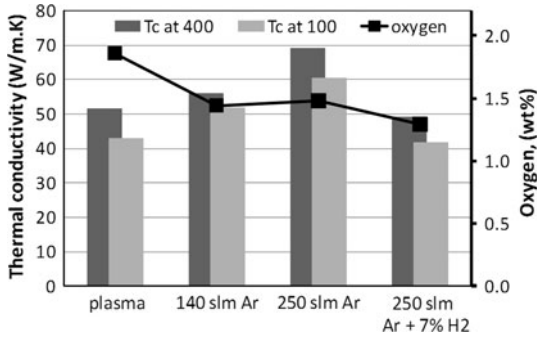

Fig. 14 Effect of shroud gas on thermal conductivity and oxygen content in Cu coatings (I = 300 A, Ar = 24 slm)

Figure 14 illustrates the effect of different shrouding regimes on the oxygen content and thermal conductivity of copper coatings. The regimes included no shrouding, two levels of shroud gas (Ar) flow rate, and an $Ar + H_2$ mixture, expected to have an added reducing effect. For pure argon, there is a clear trend of increasing thermal conductivity with shroud gas flow rate. The use of an $Ar + H_2$ mixture resulted in the lowest oxygen content, but the conductivity was similar to the unshrouded case. The graph in Fig. 14 and comparison of Fig. 12 and 13 suggest a correlation between these two quantities (lower oxygen content—higher thermal conductivity), but it does not hold universally for all coatings. Other factors, such as volume, size and shape of the voids and degree of intersplat bonding play a role here. A statistically more significant pool of data would be necessary to properly assess these relationships.

Porosity volume and Young's modulus of these coatings were also evaluated (using the same techniques as in Ref 11), but the trends were generally less distinct than for the oxygen content and thermal conductivity presented above. The latter is considered the most relevant characteristics for the prospective applications.

4. Conclusions

Copper and tungsten powders were sprayed by a hybrid torch with combined water-argon stabilization. All three studied parameters, i.e. torch power, argon flow rate and location of particle injection, were found to have a significant influence on the in-flight particle behavior. Their effects on particle velocity were generally more pronounced than effects on particle temperature. The in-flight particle temperature measurement might have been influenced by evaporation of the newly formed oxides on the particle surfaces due to reaction of the molten material with free oxygen entrained from the surrounding atmosphere. Evaluation of collected splats showed that for copper full melting of the particles took place for all studied conditions, while tungsten particles were completely molten only for conditions with high plasma enthalpy. The changes in particle state were reflected in properties of the resultant coatings, particularly their oxide content and thermal conductivity. Application of inert gas shrouding generally led to reduction in oxide content and improvement in thermal conductivity. This effect was more pronounced for copper than for tungsten. Further investigations are underway.

Acknowledgments

The authors gratefully acknowledge the financial support of Czech Ministry of Industry and Trade under project No. FR-TI2/702 and No. FR-TI2/561.

References

1. S. Sampath, X. Jiang, A. Kulkarni, J. Matějíček, D.L. Gilmore, and R.A. Neiser, Development of Process Maps for Plasma Spray: Case Study for Molybdenum, *Mater. Sci. Eng. A*, 2003, **348**(1-2), p 54-66
2. V.V. Sobolev and J.M. Guilemany, Oxidation of Coatings in Thermal Spraying, *Mater. Lett.*, 1998, **37**(4-5), p 231-235
3. M. Jankovic, J. Mostaghimi, and V. Pershin, Design of a New Nozzle for Direct Current Plasma Guns with Improved Spraying Parameters, *J. Therm. Spray Technol.*, 2000, **9**(1), p 114-120
4. K. Voleník, F. Hanousek, P. Chráska, J. Ilavský, and K. Neufuss, In-Flight Oxidation of High-Alloy Steels During Plasma Spraying, *Mater. Sci. Eng. A*, 1999, **272**, p 199-206

5. G. Mauer, R. Vassen, and D. Stöver, Controlling the Oxygen Contents in Vacuum Plasma Sprayed Metal Alloy Coatings, *Surf. Coat. Technol.*, 2007, **201**(8), p 4796-4799
6. J. Matějíček, P. Chráska, and J. Linke, Thermal Spray Coatings for Fusion Applications—Review, *J. Therm. Spray Technol.*, 2007, **16**(1), p 64-83
7. J. Matějíček and R. Mušálek, Processing and Properties of Plasma Sprayed W + Cu Composites, Thermal Spray Crossing Borders, *Proceedings of International Thermal Spray Conference*, E. Lugscheider, Ed., (Maastricht), DVS Verlag, 2008, p 1412-1417
8. J. Matějíček, V. Weinzettl, E. Dufková, V. Piffl, and V. Peřina, Plasma Sprayed Tungsten-Based Coatings and their Usage in Edge Plasma Region of Tokamaks, *Acta Technica CSAV*, 2006, **51**(2), p 179-191
9. M. Hrabovský, V. Kopecký, V. Sember, T. Kavka, O. Chumak, and M. Konrád, Properties of Hybrid Water/Gas DC Arc Plasma Torch, *IEEE Trans. Plasma Sci.*, 2006, **34**(4), p 1566-1575
10. C. Moreau, P. Gougeon, M. Lamontagne, V. Lacasse, G. Vaudreuil, and P. Cielo, On-line control of the Plasma Spraying Process by Monitoring the Temperature, Velocity and Trajectory of In-Flight Particles. *Proceedings of 7th National Thermal Spray Conference* (Boston), ASM International Materials Park, 1994, p 431-436
11. T. Kavka, J. Matějíček, P. Ctibor, A. Mašláni, and M. Hrabovský, Plasma Spraying of Copper by Hybrid Water-Gas DC Arc Plasma Torch, *J. Therm. Spray Technol.*, 2011, **20**(4), p 760-774
12. http://www.webelements.com/
13. Y.R. Niu, D.Y. Hu, H. Ji, and X.B. Zheng, In-Flight Behaviors and Properties of Plasma-Sprayed Tungsten Coatings, *Materials Science Forum*, 2010, **658**, p 13-16
14. T. Kavka, A. Mašláni, V. Kopecký, M. Hrabovský, and O. Chumak, Interaction of Thermal Plasma Jet Generated by Hybrid Gas-Water Torch with the Surrounding, *Proceedings of ICPIG-29*, Institute of Physics (IoP), July 12–17, 2009, Cancun, Mexico
15. T. Kavka, A. Mašláni, V. Sember, V. Kopecky, O. Chumak, and M. Hrabovsky, Experimental investigation of fully turbulent plasma jet and its interaction with ambient air, *Proc. ISPC-18,*(ed.) K. Tachibana, O. Takai, K. Ono, T. Shirafuji, International Plasma Chemistry Society, August 26-31, 2007, Kyoto, Japan, pp 1-4
16. J. Matějíček, O. Chumak, M. Konrád, M. Oberste-Berghaus, and M. Lamontagne, The Influence of Spraying Parameters on In-Flight Characteristics of Tungsten Particles and the Resulting Splats Sprayed by Hybrid Water-Gas Stabilized Plasma Torch, *Thermal Spray Connects: Explore Its Surfacing Potential*, E. Lugscheider, Ed., May 2–4, 2005 (Basel, Switzerland), DVS, 2005, p 594-599